npj | clean water

www.nature.com/npjcleanwater

ARTICLE OPEN

Check for updates

Efficient PFOA removal from drinking water by a dual-functional mixed-matrix-composite nanofiltration membrane

Mohit Chaudhary[1], Michal Sela-Adler[1], Avner Ronen[1]✉ and Oded Nir[1]✉

Drinking water contamination by per- and polyfluorinated alkyl substances (PFAS) is a global concern. Nanofiltration is a promising PFAS removal technology due to its scalability and cost-effectiveness. However, nanofiltration cannot typically reduce PFAS concentrations below current drinking water recommendations. To enhance PFAS removal, we developed mixed-matrix-composite nanofiltration (MMCNF) membranes—an active nanofiltration layer on porous adsorptive support that synergetically combines filtration and adsorption. We synthesized MMCNF membranes comprising thin polyelectrolyte multilayer films deposited on thick (~400 µm) polyethersulfone supports incorporating β-cyclodextrin microparticles. These membranes achieved near complete removal (>99.9%) of model PFAS (PFOA: perfluorooctanoic acid) for significantly longer filtration times compared to a control membrane without β-cyclodextrin, but otherwise identical. The spent MMCNF membrane was regenerated using ethanol, and high PFOA removal performance was regained during three filtration cycles. Perfluorooctanoic acid was concentrated 38-fold in the ethanol eluent. Further concentration by evaporation is straightforward and can enable eluent recycling and effective PFAS removal.

npj Clean Water (2023)6:77 ; https://doi.org/10.1038/s41545-023-00286-2

INTRODUCTION

In the last few decades, per and polyfluoroalkyl substances (PFAS) have been detected in drinking water at varying concentrations[1–4] resulting from various industrial and commercial sources (e.g., nonstick coating, fire-fighting foams, etc.)[4]. PFAS are persistent organic micropollutants considered potentially harmful to human health at very low concentrations (in the range of parts per trillion)[3,5]. They were shown to affect the immune system and are associated with a higher incidence of infectious diseases and varying cancer species[6]. To minimize the risk of PFAS exposure through drinking water, different regulatory agencies are developing regulations for maximum levels of PFAS in drinking water (as specific compounds and when addressed as the total PFAS concentration). The most environmentally abundant and regulated PFAS are perfluorooctanoic acid (PFOA) and perfluorobutane sulfonic acid (PFOS). In addition, the evidence showing adverse health impacts is the most established for these two compounds[3]. According to the United States Environmental Protection Agency (US EPA), the maximum concentrations of PFOA and PFOS in drinking water should be less than 70 ng L^{-1}, and according to the EU 2020 advisory for PFOA and PFOS is 100 ng L^{-1}[7,8]. The maximum allowed concentration was recently modified (US EPA 2023) to a stricter value of 4 ng L^{-1} for PFOS and PFOA[9]. Unfortunately, the most common technologies used by water treatment facilities (e.g., coagulation, sand filtration, etc.) have an insignificant impact on PFAS concentrations[10,11].

Various technologies have been developed and demonstrated for PFAS removal from aqueous systems[2,5,12–15], e.g., adsorption, oxidation, photolysis, UV degradation, and membrane separation. Among these technologies, membrane separation and adsorption stand out as practical and cost-effective[2,16]. Reverse osmosis (RO) and nanofiltration (NF) membranes can remove and concentrate most PFAS species. RO was shown to remove more than 99% of PFAS, while NF was shown to remove only 70–99%, depending upon membrane characteristics, type of PFAS, and operating conditions[2,17–20]. Although effective, membrane separation has critical limitations. While RO membranes present higher PFAS rejection, they require more energy (higher applied pressure) due to their higher density and salt rejection (higher osmotic pressure gradient)[3,6]. Conventional polyamide-based NF membranes typically remove 70 to 90%, often insufficient to meet drinking water quality regulation[7,18,19,21]. The widely studied and recently commercialized tunable, chemically stable, and antifouling NF membranes—based on multilayer assembly of polyelectrolytes—also give similar insufficient PFAS rejection (60 to 90%)[22].

In addition to membrane rejection, PFAS adsorption was performed using a range of adsorbers, including activated carbon, ion exchange resins, etc.[3,23] Recently, cross-linked β-cyclodextrin-based adsorbents[24,25] were reported to exhibit high removal, an exceptionally high uptake rate, and good regeneration potential. These properties can be attributed to unique cavities of ~0.78 nm size that work at the molecular level to capture PFAS by size inclusion mechanism while excluding larger molecules by size exclusion. Further surface charge imparted by functionalization also enhances the affinity for adsorbates via electrostatic interactions[26,27]. Currently, the main restriction of using β-cyclodextrin for PFAS removal is the competition with organic matter and the need for frequent sorbent regeneration or replacement[24,27]. In this work, we overcome the limitations of both filtration and adsorption by hybridizing these technologies.

Heretofore, coupling of adsorption with membrane filtration was studied mainly as separate process steps[2,12,24] or by incorporating the adsorbent in the membrane's active layer[28,29]. A recent study used mixed-matrix composite nanofiltration membranes containing poly-N-isopropylacrylamide (PNIPAm) functionalized microfiltration support layer[30]. This dual-functional adsorptive nanofiltration membrane showed a rejection of only 70% for PFOA. Moreover, PFOA desorption and recovery were not

[1]The Department of Desalination & Water Treatment, Zuckerberg Institute for Water Research, Blaustein Institutes for Desert Research, Ben Gurion University of the Negev, Sde Boker 84990, Israel. ✉email: avnerr@bgu.ac.il; odni@bgu.ac.il

explored. Thus, the development of regenerable mixed-matrix nanofiltration membranes with very high PFAS removal is in need to treat drinking water according to the increasingly strict regulations. Various studies have introduced mixed-matrix membrane/hybrid membranes to remove different organic micropollutants through selective adsorption. However, due to early saturation of the adsorbent's active sites, difficulty in regeneration, dependence on feed pH, and low hydraulic residence time, these membranes were not found commercially viable[29–31].

Here, we fabricated a novel mixed-matrix composite NF membrane (MMCNF). The membrane included an asymmetric polyethersulfone (PES) support layer wherein β-cyclodextrin adsorbent microparticles were embedded. On top of the mixed matrix support, a multilayer polyelectrolyte NF thin film was deposited. Conceptually, this membrane can remove PFAS by two mechanisms: (1) rejection by the active NF layer; and (2) adsorption on the Dexsorb® particles incorporated in the active and support layers (Fig. 3b). We chose the PDADMAC-PSS polyelectrolyte assembly due to its low swelling at ambient pH[32] and good chemical stability[33]. We selected PFOA as a model for long-chain PFAS because it is highly abundant in groundwater; its impacts on health and the environment were extensively studied, and it is regulated in the United States and Europe[4,6,7,10,18]. More details related to the physicochemical properties of PFOA has been provided in the supplementary data[3,34] (Supplementary Table 4). Compared to the control, PFOA removal by the MMCNF was dramatically enhanced and remained very high through several filtration-regeneration cycles. We used ethanol[25] to extract the adsorbed PFOA and regenerate the MMCNF. The extracted PFOA was at a higher concentration in the ethanol solution, facilitating more economical disposal or destruction of these chemicals.

RESULTS AND DISCUSSION

Membranes characterization

Dexsorb®, a commercial adsorbent for micropollutants delivered as cross-linked β-cyclodextrin microparticles (more details in the "Materials and chemicals" section), was embedded in the MMCNF membranes' support layer. The membranes were prepared with three different mass loadings of Dexsorb® particles (Table 1), 0% (M0), 6% (M6), and 8% (M8). Loadings greater than 8% resulted in a non-usable brittle support layer due to the size of the adsorbent particle (see below) and the high viscosity of the casting mixture. SEM images (Fig. 1) confirmed the successful incorporation of Dexsorb® into the membrane. Plan view image of the M0 surface (Fig. 1a) showed a smooth surface typical to a layer-by-layer assembly of polyelectrolytes[35], and the cross-section image of M0 (Fig. 1b) revealed the asymmetric sponge structure typical to PES ultrafiltration membranes (fabricated through non-solvent-induced phase separation). No particles appear on either image. In contrast, plan view and cross-section SEM images of membranes M6 and M8 (Fig. 1c–f) revealed distinct particles on the membrane surface and within the porous support. The embedded particles were uniformly distributed, and their observed density was higher for the membrane with the higher β-cyclodextrin loading (M8) as expected. The particle sizes observed in the SEM micrographs agree with the 1–20 µm size distribution, measured independently in suspension via electrical zone sensing (Supplementary Fig. 2). The similarity in particle diameters indicates that no significant aggregation of β-cyclodextrin occurred.

Table. 1. Composition dope solution for the preparation of M0, M6, and M8 membranes.

Membrane	PES (wt% of dope solution)	Dexsorb® (wt% of dope solution)	NMP solvent (%)
M0	17	0	83
M6	17	6	77
M8	17	8	75

The incorporation of β-cyclodextrin particles affected the properties of the PES support layer and the active NF surface layer. In M0, the SEM imaging revealed macro voids underneath the skin layer (Fig. 1b), while M6 and M8 had a more unidirectional micropore structure (Fig. 1d, f). This structural difference may be attributed to the delayed mass transfer and solvent and non-solvent demixing during the MMCNF membrane casting process[18,19]. A decrease in void volume was confirmed by measuring the bulk porosity (Fig. 2a), which was slightly lower for the MMCNF membranes compared to the pure PES. Surface-bound β-cyclodextrin particles affected the MMCNF surface roughness and charge. The surface roughness of M8 was higher than M0 and had a greater variance, as indicated by the root mean square roughness (R_q) measured using AFM (Fig. 2c). Lower negative surface charge (zeta potential) was recorded for M0 compared to M6 and M8 (Fig. 2b) at ambient pH range (5–9). This loss of negative charge is due to the commercial sorbent being a mixture of positively charged and neutral β-cyclodextrin particles.

The embedded β-cyclodextrin particles also affected the filtration performances of the MMCNF membranes. The pure water permeance increased with increased particle mass load (Fig. 2d), reaching a ~28% increase for M8 compared to M0. The increased permeance suggests a looser structure of the polyelectrolyte multilayer, which may be attributed to the increased surface roughness (Fig. 2b) caused by near-surface particles. The MWCO of the NF membranes also increased (by 5%) with particle loading (Fig. 2e), indicating increased effective pore size and affirming a looser active layer structure for MMCNF membranes. Further support for a more open structure was obtained from the decrease in Na_2SO_4 rejection with increased particle loading (Fig. 2e). Na_2SO_4 passage increased from 9% to 15%, which may be partly attributed also to the smaller negative surface charge (Fig. 2b) in the MMCNF membranes. A higher salt passage is advantageous in drinking water NF applications due to (1) lower salinity of the brine, (2) lower energy requirements, and (3) maintaining essential minerals in the permeate. In summary, the β-cyclodextrin particles embedded in the support improved membrane permeance and increased the salt passage while only slightly affecting neutral solute MWCO.

PFOA retention improved upon increasing adsorbent loading

Preliminary experiments with high PFOA feed concentrations (161–345 µg L^{-1}) revealed that higher loadings of β-cyclodextrin significantly increased PFOA removal efficiency (Fig. 3a). Filtration experiments were carried out with loadings of 0% (M0), 6% (M6) and 8% (M8) w w^{-1} (Table 1), using a typical filtration setup (Supplementary Fig. 1) operating in a full recirculation mode. During the first 3 h of filtration, the control (M0) membrane achieved PFOA removal of ~97%, but afterward, the rejection declined, reaching about 73% after 20 h. Using the M6 membrane, PFOA concentration in the permeate was below the detection limit (1 µg L^{-1}) for 10 h, represented as 100% removal (Fig. 3a). After 20 h, PFOA was detected in the permeate at a low concentration corresponding to ~99.7% removal and the removal declined to ~99% after 33 h. For the membrane with the highest loading, M8, the removal was greater than 99.9% throughout the experimental time (33 h). These preliminary results pointed to the potential of the MMCNF concept as an effective barrier for PFAS.

Adsorption and saturation of PFOA in the membranes partly explain the PFOA removal trends (Fig. 3a). As illustrated in Fig. 3b, PFOA removal occurs via two mechanisms: (1) rejection by the NF

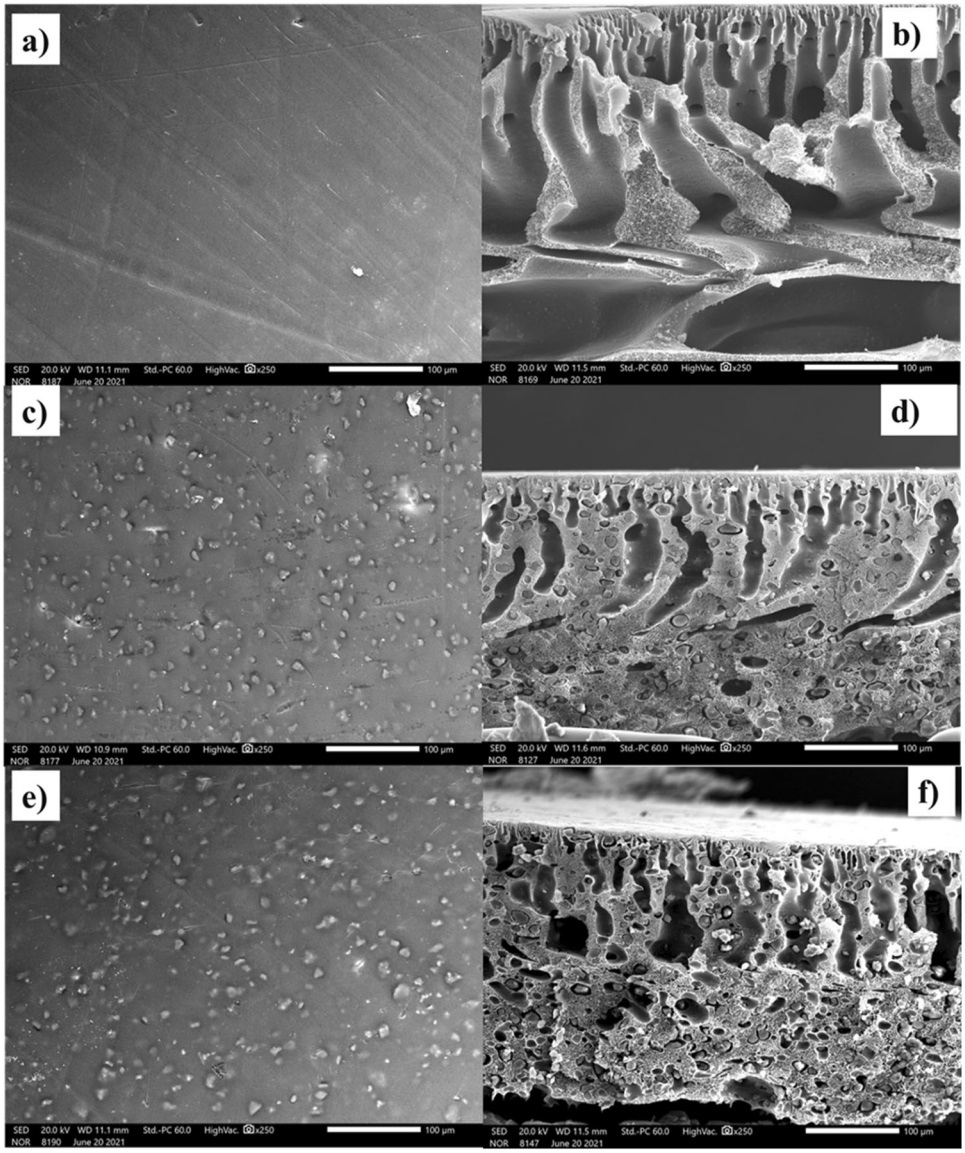

Fig. 1 SEM images of control (M0) and mixed matrix composite nanofiltration membranes. SEM micrographs showing cross-sectional and top surface morphologies of M0 (**a**, **b**) the control membrane, M6 (**c**, **d**) having 6% sorbent loading, and M8 (**e**, **f**) having 8% sorbent loading. Uniformly distributed β-cyclodextrin microparticles (1–20 µm) appear embedded on the top surface and inside the membrane matrix. The particle density increases with sorbent loading and is highest for M8. The support layer void volume seems lower in MMCNF membranes compared to the control membrane.

layer; and (2) adsorption either in the NF layer or the porous support. Consequently, the removal data exhibit a 'breakthrough curve' pattern (note that this is not a classic breakthrough experiment) that depends on the NF layer base-level rejection, adsorption capacity, and kinetics. Batch adsorption results (Supplementary Table 1 & Supplementary Fig. 6) revealed that the M8 adsorption capacity for PFOA (5368 µg g^{-1} of membrane) was higher than that of M0 (5.99 µg g^{-1} of membrane) by a factor of almost 1000. In M8, PFOA was mainly adsorbed on the β-cyclodextrin embedded in the PES support and exposed to the permeating water (we approximated that *at least* 7% of the total sorbent mass was exposed to the water, see details in the Supplementary Note 3 of supplementary information file). In contrast, in M0 (which has no β-cyclodextrin), only the pDADMAC-PSS active layer or the PES could provide adsorption sites for PFOA[36–38]. Accordingly, PFOA saturation occurred faster for M0, leading to the early drop in the PFOA removal rate until reaching a steady state at ~73%. In contrast, M8 achieved almost complete removal throughout the experiment. For M6, PFOA removal declined earlier than M8 due to its lower β-cyclodextrin loading but was still higher than M0, supporting the filtration-adsorption explanation. The fact that the removal remains high in the MMCNF membranes is addressed at the end of this section. Following these results, the M8 membrane was selected for further investigations and is referred to as MMCNF below.

The MMCNF membrane achieved high PFOA removal in several filtration-regeneration cycles

In the filtration experiments described in the previous section, the high PFOA feed concentration (161–345 µg L^{-1}) enabled us to observe breakthrough behavior in practical experimental times and to compare the composite membranes accordingly. In the current sections, we tested the MMCNF performances under lower feed concentrations (~45 µg L^{-1} in Milli-Q water), such as those found in highly PFOA-contaminated groundwater[2]. Feed concentration may affect the removal efficiency depending on the

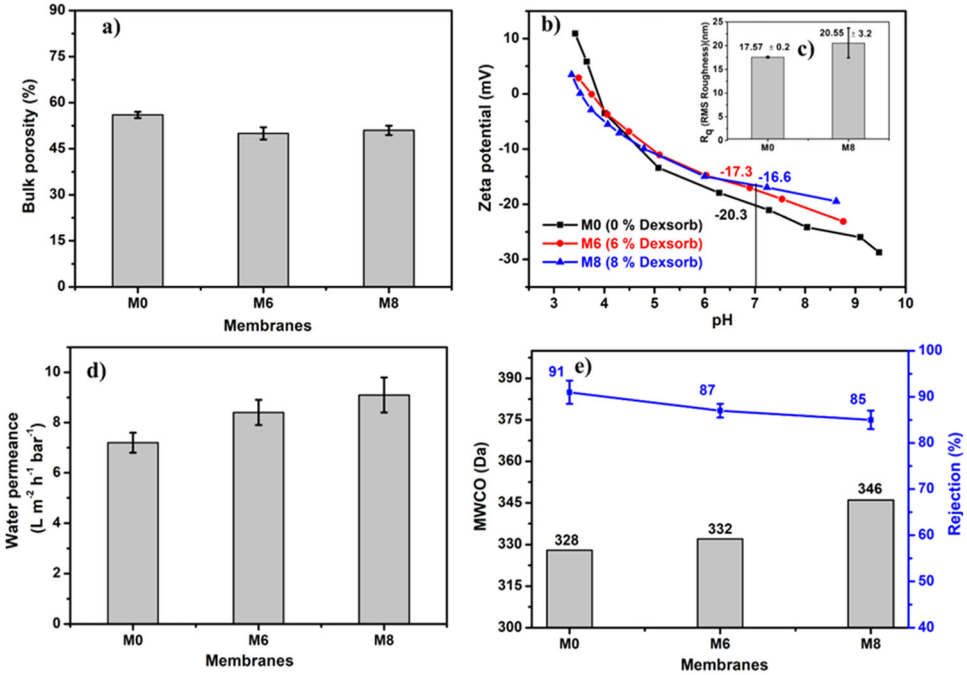

Fig. 2 Characterization of control (M0) and mixed matrix composite nanofiltration membranes. Bulk porosity (**a**), surface zeta potential (**b**), root-mean-square (RMS) surface roughness measured by atomic force microscopy (**c**), water permeance (**d**), molecular weight cutoff (MWCO), and Salt rejection (**e**) of control (M0) and MMCNF membranes. For all filtration experiments, the operating pressure was 2 bar, the temperature was 25 °C, and the crossflow velocity was 10.2 cm s^{-1}. Sodium sulfate concentration was 1 mM. All measurements were performed in triplicates, and the average value is shown with standard deviations as error bars.

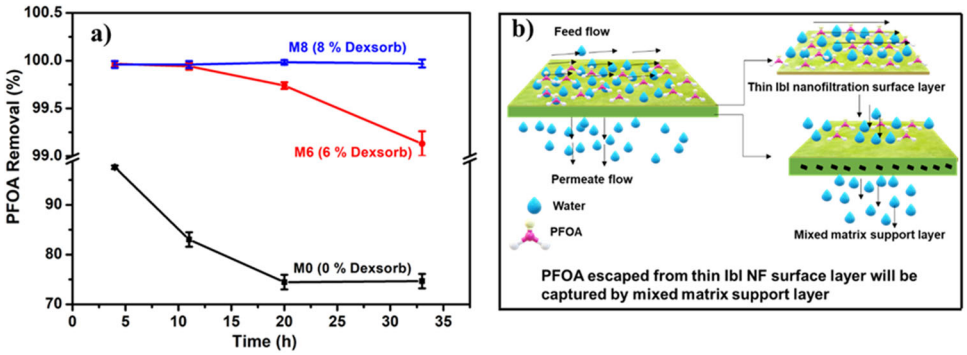

Fig. 3 Effect of Dexsorb® loading and illustration of PFOA removal mechanisms. a Impact of adsorbent loading on the time-dependent PFOA removal performance; and **b** conceptual representation of the dual-functionality filtration process. Filtration experiments were performed in a crossflow filtration setup with recirculation of the feed and permeate streams. Experimental conditions: Operating pressure: 2 bar, Temperature: 25 °C, Feed: PFOA spiked milli-Q for M6, M8, M0: 345 µg L^{-1}, 285.5 µg L^{-1}, and 161 µg L^{-1}, respectively. Permeate flux during M0, M6, and M8 membrane run: 6.5, 7.7, and 8.7 $Lm^{-2}h^{-1}$ bar^{-1}, respectively. When PFOA concentration was below the detection limit in this experiment (0.5 µg L^{-1}), the removal was set to 100%. The error bars represent the error in the analytical method, determined using our quality assurance process (see "Methods" for more details). Briefly, it is the standard deviation around the mean ($n = 3$) of measured values of verified standards.

adsorption isotherm and kinetics. Demonstrating high removal at different feed concentrations during longer operation times is imperative.

The highly effective PFOA removal by the M8 MMCNF membrane was maintained in four consecutive cycles during the entire filtration time (Fig. 4). We conducted four filtration-regeneration cycles using the same membrane. Ethanol was used for PFOA desorption due to its lower toxicity than methanol used in previous studies[39]. PFOA removal was consistently greater than 99.8% during the 1st and 2nd cycles for 160 and 185 h, respectively (Fig. 4a, b). In the 3rd and 4th cycles (Fig. 4c), PFOA removal slightly decreased but remained very high (99.3–99.9%). Due to the high removal rate, PFOA permeate concentrations were below the EU and EPA 2020 recommendations (0.1 and 0.07 µg L^{-1}, respectively), despite the high PFOA feed concentration (45 µg L^{-1}, much higher than in typical contaminated groundwater). A decreasing trend in the PFOA removal rate in the final stages of filtration was not observed in any cycle, indicating that vacant adsorption sites remained. Extrapolation of these results to a more typical (yet still high) groundwater PFOA concentration (e.g., 0.5 µg L^{-1}) suggests an effective removal for over two years can be achieved before regeneration is needed.

High PFOA removal efficiency was maintained during filtration and after regeneration throughout all cycles, indicating that the MMCNF was stable in water and ethanol (Fig. 4a–c). In the 4th cycle, the initial removal rate was lower but later recovered.

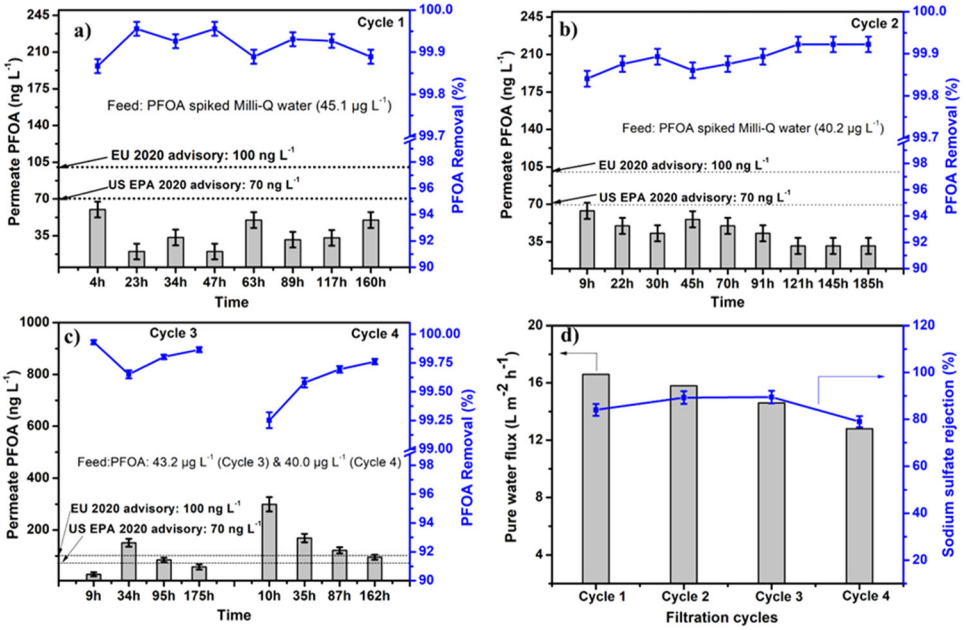

Fig. 4 PFOA removal from spiked Milli-Q water during four filtration cycles. PFOA removal and permeate concentration during **a** cycle 1; **b** cycle 2; and **c** cycles 3 and 4. The feed volume was 2.3 L. **d** Pure water flux and salt rejection before each cycle (measured at 2 bars). After each cycle, the MMCNF (M8) membrane was regenerated using ethanol at 2.5 bar and rinsed with Milli-Q water. MMCNF showed very high PFOA rejections (~99.9%) up to two cycles, and later a slight decrease in performance was observed, but the removal remained above 99%. The pure water flux decreased after each cycle, whereas salt rejection did not show a clear trend. The error bars represent the error in the analytical method, determined using our quality assurance process (see "Methods" for more details). Briefly, it is the standard deviation around the mean ($n = 3$) of measured values of verified standards.

Filtration experiments using (i) milli-Q water and (ii) 1 mM Na_2SO_4 after each cycle showed a decline in pure water flux (~25%), whereas the salt rejection did not show a significant trend. Interestingly, immersing the membrane in ethanol for four days resulted in an opposite trend, i.e., a 25% increase in pure water flux (Supplementary Fig. 7), while the salt rejection decreased by 9%, consistent with the filtration experiments. Ethanol was previously found to affect the interactions in PSS-PDADMAC complexes[40], which may lead to condensation of the assembled layers. In contrast, concentrated salt solutions loosen the layer and may even remove it[41]. Therefore, after regeneration with ethanol, the active layer performances can be restored simply by applying a salt solution that will modify the existing layer or remove and redeposit as previously proposed[41]. Indeed, a preliminary experiment we conducted revealed that the water permeance and salt rejection increased after treatment with 3 M NaCl (see results and details in Supplementary Table 3). We plan to adopt this protocol after regeneration and optimize it in future studies.

High PFOA removal was maintained for spiked tap water

When using the MMCNF to treat PFOA-spiked tap water, the removal rate was very high in three consecutive filtration-regeneration cycles, despite competing inorganic ions[17] and other trace organics (Fig. 5a, b). A reproducible breakthrough behavior, typical to adsorption, was observed after ~45 h for the 1st and 3rd cycles and ~32 h for the 2nd cycle. This reproducibility suggests that the composite membrane is stable and no significant leaching occurs. The breakthrough behavior can be related to the higher PFOA feed concentration (~500 µg L^{-1}) used in tap water, which was ~10-fold higher than in the DI experiments depicted in Fig. 4. The first 45 h, in which the MMCNF membrane achieved 99.9% PFOA removal, translates to ~712 L (calculated by multiplying the average flux, 15.8 Lm^{-2} h^{-1}, by the time, 45 h) of treated drinking water for every m^2 of the membrane (Fig. 5a) before regeneration is needed. For a more typical PFOA concentration in contaminated groundwater (e.g., 0.5 µg L^{-1}, ~1000 times lower than the feed concentration used here), the water volume per m^2 is expected to increase significantly due to the lower PFOA loading and lower required removal (to meet the regulations). Higher water volumes per m^2 of membrane translates into long operation time before regeneration is needed.

Low eluent volume in the desorption step resulted in a concentrated PFOA-in-ethanol solution. Concentrating PFOA from a diluted source could facilitate cheaper and more effective destruction or disposal. Similar to the DI experiments, regeneration after spiked tap-water filtration fully restored the membrane adsorption capacity. PFOA removal rate returned to the high initial value after each regeneration step (Fig. 5b), indicating successful desorption, further affirmed by the high PFOA concentration in the ethanol eluent (Fig. 5d). The regeneration step did not significantly affect the salt rejection. At the same time, pure water permeance decreased by ~30% (Supplementary Fig. 8), whereas the average water flux during the filtration steps only reduced by 12% (Fig. 5c). Mass balance revealed that PFOA was concentrated in ethanol by a factor of 10-38 compared to the feed, with a 29% PFOA surplus after the 2nd cycle (Supplementary Fig. 9a) and a 19% deficit after the 3rd cycle (Supplementary Fig. 9b). These discrepancies may be related to adsorption/desorption from tubing or analytical issues. We expect much higher concentration factors would be attainable for a lower eluent-volume to membrane-surface area ratio and lower PFOA feed concentration, which requires long-duration experiments and a higher membrane surface area than reported here. These results indicate that practically all PFOA can be desorbed from the membrane and concentrated in a lower volume ethanol solution in significantly shorter times than the filtration time, restoring the PFOA removal performances in the next cycle. Optimization of the regeneration step is planned for future studies.

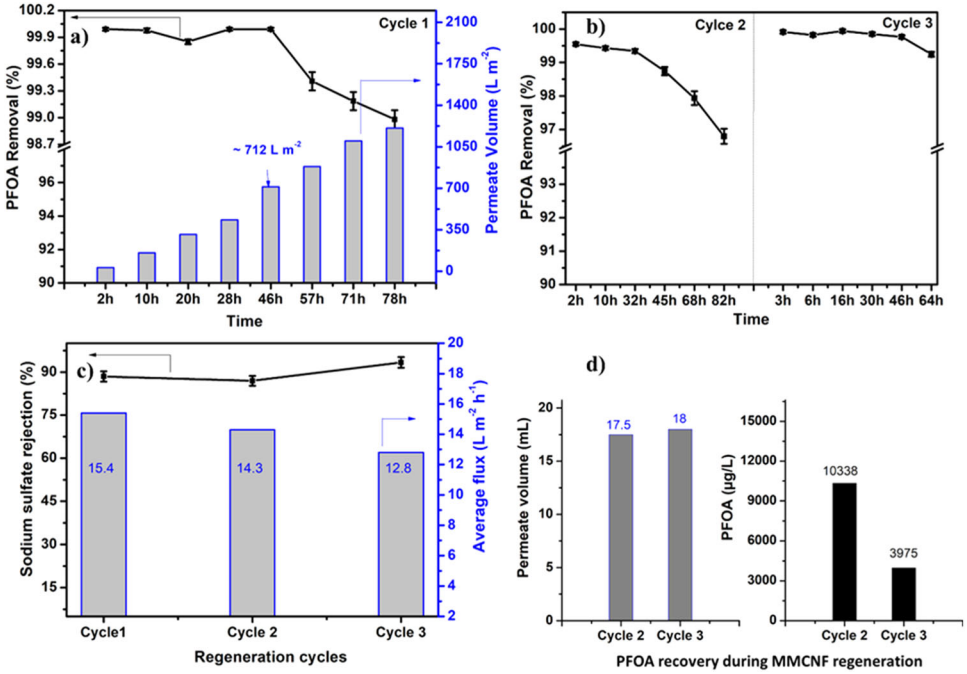

Fig. 5 PFOA removal from spiked tap water and membrane regeneration. a Permeate volume and PFOA retention during spiked tap water experiment (cycle 1), **b** PFOA removal performance during two additional consecutive cycles after regeneration. In all cycles, PFOA removal >99% was recorded before the breakthrough occurred, suggesting that regeneration before the breakthrough can maintain constant high PFOA removal. **c** Average permeate flux during each cycle and salt rejection before each cycle. **d** Characteristics of permeate collected during the MMCNF regeneration experiment after cycle 2 and cycle 3. Feed PFOA concentrations during cycles 1, 2, and 3 were 540, 334, and 344 µg L^{-1}, respectively. During cycle 1, the treated volume was estimated based on average flux (15.4 Lm^{-2} h^{-1}). The error bars represent the error in the analytical method, determined using our quality assurance process (see "Methods" for more details). Briefly, it is the standard deviation around the mean ($n = 3$) of measured values of verified standards.

PFOA adsorption enhances its rejection by affecting the membrane surface charge

As more PFOA adsorbed to the membrane, the estimated rejection by the NF layer gradually increased to 77% and fluctuated within the range of 60–73%, which is similar to the steady state removal of the control NF (M0, Fig. 3a). The results thus suggest that in long-term filtration, ~70% of PFOA will remain in the concentrate, ~30% will be adsorbed and ~0.1% will pass to the permeate. Optimizing the NF active layer for higher PFAS rejection can prolong the time between regeneration steps. We propose that the increasing rejection of PFOA by the NF active layer (Fig. 6a) is partially due to enhanced negative surface charge induced by PFOA adsorption (Fig. 6c). PFOA molecules are negatively charged at ambient pH[27] and can be electrostatically adsorbed to the positively charged quaternary ammonium groups in the polyelectrolyte layer (the polyDADMAC's charge that the PSS did not neutralize). PFOA adsorption, therefore, induces excess negative charge, which is confirmed by zeta potential measurements of unused and spent M0 (Fig. 6b). In the MMCNF membrane, PFOA also adsorbs to the surface-bound Dexsorb® sorbent (Fig. 1c, e). The latter is a mix of positively charged and neutral particles, which adsorbs PFOA through electrostatic and hydrophobic interactions. Therefore, the increase in surface charge following PFOA adsorption is more prominent for M8 (Fig. 6b), likely contributing to higher electrostatic repulsion[17] of anions. Another possible explanation for the increase in PFOA rejection is its adsorption on the surface and within the NF active layer. The occupation of adsorption sites could hinder the passage of PFOA through the NF layer, and this mechanism can operate together with electrostatic effects.

Significance and prospects

In previous studies, commercial and lab-made nanofiltration membranes achieved 80–99% PFOA rejection, depending on membrane characteristics and other operating conditions[18,19,21,22,30] (Table 2). The dual-function MMCNF membrane developed in this study showed markedly improved PFOA removal 99.9%, a ten-fold decrease in PFOA permeate concentration compared to 99% rejection. The removal was in-par with removal by reverse-osmosis membranes with the advantage of generating a lower salinity retentate, thus saving energy and brine treatment costs. The MMCNF developed here also significantly exceeds the performance of a recently introduced dual-functional membrane[30], which achieved 70% PFOA removal. Moreover, the membrane was reusable after a simple regeneration cycle. Therefore, our dual-functional MMCNF membrane is a significant step forward in PFAS removal technology from drinking water.

The composite mixed-matrix membrane synthesis approach presented in this work can be further optimized and adjusted for treating a wide range of microcontaminants. Porous PES filters (used in this study) support the thin active film in most commercial composite membranes and many novel ones. Therefore, the active layer can be modified based on separation needs, e.g., denser NF/RO layers for short-chain PFAS or looser NF layer, or even no layer for larger PFAS or other microcontaminants. Specifically, polyelectrolyte multilayer deposition (used here) is a flexible and tunable approach that can be optimized to achieve desired membrane performance. Further performance enhancements can be expected from optimizing the embedded sorbent. Furthermore, using nanoparticles instead of microparticles could improve adsorption capacity and kinetics, allowing even higher contaminant removal for longer filtration cycles. Beyond that, the

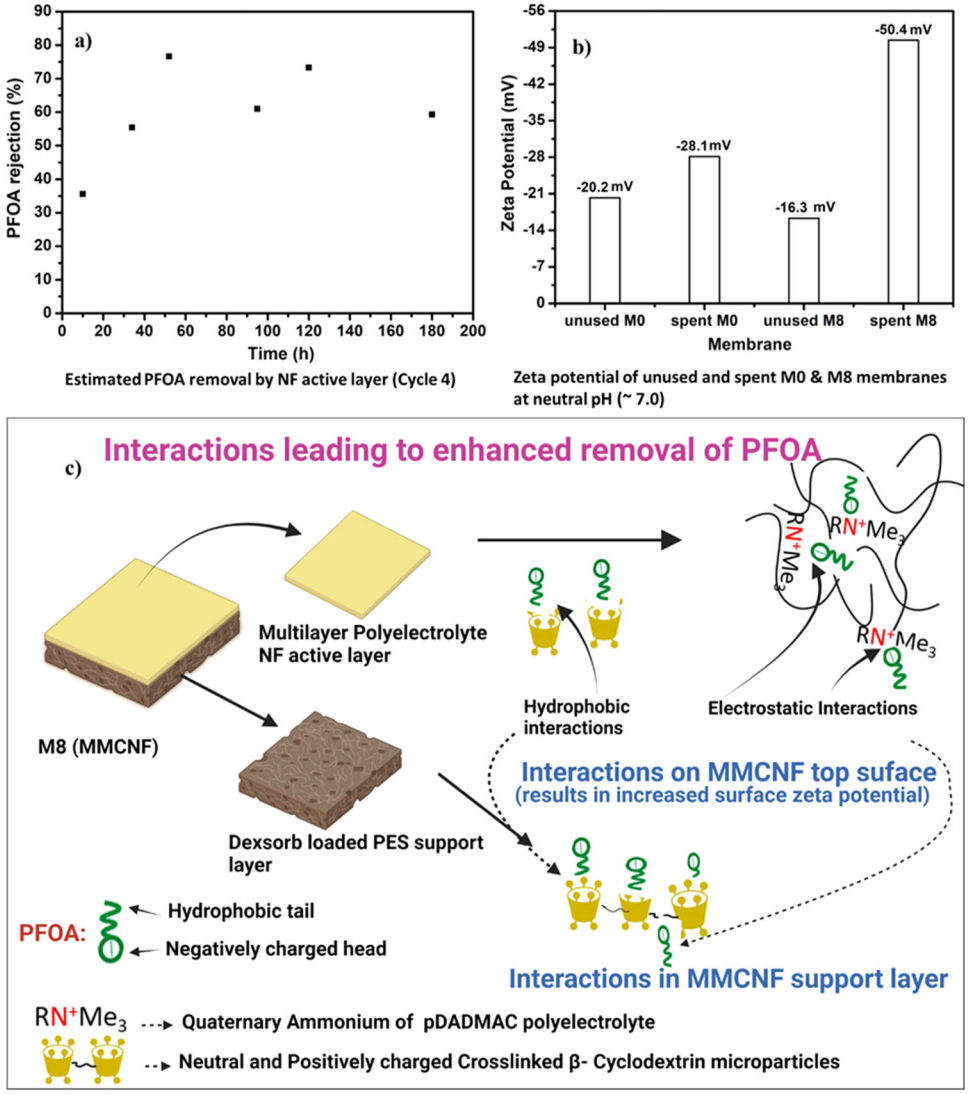

Fig. 6 Quantitative investigation of PFOA removal mechanisms. a Estimated PFOA removal by the NF active layer. **b** Surface zeta potential of virgin and spent MMCNF showing an increase in surface zeta potential for spent M0 and MMCNF membranes. **c** Illustration of the interactions leading to the enhanced removal of PFOA.

Table. 2. Comparison of the current work with similar recently published work on PFOA removal by reverse osmosis and nanofiltration membranes.

Membrane type[ref]	MWCO/pore diameter	Filtration Experiment Unit	Feed PFOA (μg L^{-1})	Water permeance ($Lm^{-2}h^{-1}bar^{-1}$)	Water Matrix and maximum PFOA removal (%)
Polyamide NF (lab)[19]	1.2 nm	Crossflow	1000	~12	DI water- 90
NF 270 (commercial)[19]	0.8 nm	Crossflow	1000	~21	DI water- 90
Fully aromatic polyamide advanced composite membrane (commercial)[18]	200 Da	Crossflow	5, 50, 100	~5	DI water- 97.3–99.85 Spiked groundwater- 99.54
SiO_2/CMWCNT/PMIA hollow fiber NF (Lab)[21]	661 Da	Crossflow	25-100	–	DI Water- 95.3 to 98.3
Poly-N-isopropylacrylamide (PNIPAm) pore-functionalized microfiltration support-based NF (Lab)[30]	–	Crossflow	70	~12	DI water + 2 mM $CaCl_2$- 70
Polyelectrolyte (PDADMAC, PSS) multilayer nanofiltration membranes[22]	–	Crossflow	1000	~12.5	DI water- ~90 DI water + combined salts- ~90
Mixed matrix composite nanofiltration membrane (This study)	346 Da	Crossflow	45-500	~9	~99.9

sorbent type can be adjusted to target different organic and inorganic contaminants.

METHODS

Materials and chemicals

High molecular weight polyether sulfone (PES, Ultrason E6020P with MW 58000 g mol^{-1}) flakes and N-Methyl-2-pyrrolidone (NMP) solvent were used to prepare the ultrafiltration support layer. A mixture of cross-linked β-cyclodextrin polymer-based neutral and positively charged adsorbent Dexsorb® (50% Dexsorb® and 50% Dexsorb® +) with particle size <45 µm was provided by CycloPure, Encinitas, CA. The Dexsorb® was further sieved (Arilevy, Petah-Tikva, Israel) to obtain a lower particle size (<20 µm). 20% Poly diallyldimethylammonium chloride (PDADMAC) with molecular weight 400,000 to 500,000 and poly (sodium 4-styrenesulfonate) (PSS) with a molecular weight of 100,000 kDa (Sigma-Aldrich) were used to prepare polyelectrolyte multilayers. Sodium metabisulfite was used to prepare the membrane storage solution. Methanol (Bruker), Ammonium Acetate (Sigma-Aldrich), Milli-Q water (LCMS grade), 24 native compound mix (PFAC-24PAR), and labeled compound mix (MPFAC-24ES) (Wellington Laboratories, Greyhound, UK), PFOA 40% (Sigma-Aldrich) was used for PFOA measurements.

Preparation of MMCNF membrane

A (~400 µm) PES UF support layer loaded with varying concentrations of commercially available β-cyclodextrin based Dexsorb® adsorbent was fabricated using the phase inversion method. The UF membrane casting solution was prepared by dissolving PES (17 wt%) in NMP at room temperature. PES casting solution with 0, 6, and 8 wt% of Dexsorb® (from the total casting solution weight) was used to form the mixed matrix UF support. Briefly, Dexorb was added into the NMP solution while stirring at 800 rpm for 20 min. Next, PES was added to the solutions in small amounts over 2 h. The solution was stirred at 300 rpm for 24 h and left untouched for a few hours to remove air bubbles. Afterward, the casting solution was poured onto a non-woven fabric on a glass plate, and a casting blade was used to cast a ~400 µm thick membrane (thickness excluding non-woven support). The glass plate with the membrane was transferred into a water bath at 25 °C. After 2 h, the membrane was kept in Milli-Q water with 0.25 wt% sodium metabisulfite solution. The prepared support layers were named UF0, UF6, and UF8, having Dexsorb® loading of 0, 6, and 8 wt%, respectively.

Positively charged PDADMAC (1 g L^{-1} in 0.5 M NaCl solution) and negatively charged PSS (1 g L^{-1} in 0.5 M NaCl solution) were used to prepare a polyelectrolyte nanofiltration thin active layer on the mixed matrix ultrafiltration support layer. PDADMAC and PSS were selected for the preparation of the NF active layer as they are strong polyelectrolytes, stable in a wide pH range, and proven to be the appropriate pair for nanofiltration active layer preparation[42]. The NF layer was fabricated on the top of UF support layers (UF0, UF6, UF8) by depositing six PDADMAC and PSS bilayers, thus forming the MMCNF with a negative surface charge. The MMCNF were named M0 (0% Dexsorb® loading), M6 (6% Dexsorb® loading), and M8 (8% Dexsorb® loading) following the support UF membranes used. Only six polyelectrolyte bilayers were deposited for fabricating the NF active layer because, due to the deposition of more than six bilayers, excess positive charge accumulates on the membrane's surface, resulting in a lower negative surface charge[43].

Characterization of membranes

M0, M6, and M8 membranes were characterized to investigate the following properties. Surface and cross-sectional Field Emission Scanning Electron Microscope (FESEM) micrographs were obtained using a JSM-IT200 instrument (JEOL, Japan). Furthermore, the top surface morphology of the PES support and MMCNF membranes were compared using Atomic Force Microscopy (AFM) imaging by NanoWizard 4 microscope (JPK Instruments, Bruker Nano GmbH, Berlin, Germany). The membranes' Molecular weight cutoff (MWCO) was obtained using 1 g L^{-1} of Glucose (180 Da), Sucrose (354 Da), Raffinose hydrate (494 Da), and PEG 1000[44,45]. The membranes' water permeance was calculated as in Kamp et al. (2021)[42] and Wu et al. (2022)[46]. Briefly, after membrane compaction, permeate was collected at 2 bar operating pressure, and water permeance was calculated using the following Eq. 1.

$$W_p = \frac{V}{A * t * \Delta P} \quad (1)$$

where W_p is the water permeance in ($Lm^{-2}\,h^{-1}\,bar^{-1}$), V is volume (L) collected, t is time (h), A is effective membrane area (m^2), and ΔP is operating pressure.

The bulk porosity (P) of membranes was obtained using the following Eq. 2.

$$P = \frac{w_1 - w_2}{\rho * A * l} * 100 \quad (2)$$

Where w_1 and w_2 are the weights of wet and dry membranes in g, respectively, while ρ, A, and l are the density of water (g cm^{-3}), area (cm^2), and thickness of the membranes (cm), respectively. The zeta potential of the membranes at varying pH values was measured using a SurPASS electrokinetic analyzer (Anton Paar, Graz, Austria). During measurement, 10 mM KCl electrolyte solution was passed through an adjustable gap cell (at 100 ± 7 µm gap) at 400 mbar pressure.

Sodium sulfate rejection was measured using the following Eq. 3,

$$\text{Salt rejection}(\%) = \frac{C_f - C_p}{C_f} \times 100 \quad (3)$$

C_f and C_p are the feed and permeate conductivity (µS cm^{-1}), respectively.

The term 'removal' was used to distinguish it from 'rejection' by the active NF layer. High removal efficiency is simply a high value of removal, which is mathematically identical to observed rejection ($1-C_{permeate}/C_{feed}$), but is different mechanistically. So in the present study, PFOA removal (%) was calculated using the following Eq. 4.

$$\text{PFOA removal}(\%) = \frac{C_0 - C_p}{C_0} \times 100 \quad (4)$$

Where C_0 is the initial feed concentration, and C_p is the PFOA concentration in permeate at time t.

Filtration system and protocol

A crossflow membrane setup with an effective membrane area of 22 cm^2 was used to conduct the filtration experiments in full recirculation mode (Supplementary Fig. 1). Before the filtration experiment, MMCNF was conditioned by carrying out compaction at 3 bar operating pressure for 4 h. Milli-Q water was filtered through the membrane in full crossflow recirculation mode during compaction. Experimental conditions, such as operating pressure, temperature, and crossflow velocity, were kept at 2 bar, 25 °C, and 11.20 cm s^{-1} for all the filtration experiments. The permeate and concentrate were recirculated back to the feed tank. All filtration experiments were conducted at low operating pressure (at 2 bar to maximize PFOA adsorption on the support layer by increasing the contact time between PFOA and Dexsorb® particles).

The Quality Controls (0.5 µg L^{-1}, 1 µg L^{-1}, 5 µg L^{-1}, 10 µg L^{-1}, 30 µg L^{-1} PFAS standards) were placed after every ten samples during the LCMSMS run for quality assurance. Standard deviations

around the mean ($n = 3$) of measured values of verified standards were used to estimate the standard deviation for PFOA measurements. Standard deviations were plotted as error bars. We conducted all other measurements in replicates and reported the average value and standard deviations were plotted as error bars.

PFOA adsorption, rejection, and membrane regeneration

Initially, PFOA removal performances of three MMCNF membranes, M0, M6, and M8, were compared to identify the best Dexsorb® loading. The best-performing membrane (M8) was used for further PFOA adsorption, rejection, and regeneration experiments.

Batch adsorption experiments were carried out at different PFOA concentrations (100 μg L^{-1}; 250 μg L^{-1}; 500 μg L^{-1}; 1000 μg L^{-1}; 2000 μg L^{-1}; 5000 μg L^{-1}) using only PES support layer (UF0) and mixed matrix support with optimized loading (UF8) with similar area and mass (9 cm^2 of membrane weighing 0.15 g). All experiments were conducted at a stirring speed of 200 rpm, 48 h contact time, and a temperature of 25 °C. The experimental data were fitted to adsorption isotherms (see Supplementary Fig. 6) to estimate the PFOA adsorption capacity of the mixed-matrix membranes (in both mg g^{-1} and mg m^{-2}).

Rejection experiments were carried out in crossflow recirculation mode using Milli-Q water spiked with ~45 μg L^{-1} PFOA and tap water spiked with ~500 μg L^{-1} PFOA. Experimental conditions such as operating pressure, crossflow rate, and feed temperature were kept as described earlier in this section. According to equipment PFOA measurement capacity (LC-MS-MS), to estimate the permeate concentration in ppt (only for spiked Milli-Q), permeate samples were concentrated 20 times by reducing the liquid volume at 38 °C.

The stability of MMCNF towards regeneration was evaluated using ethanol (99%) at static and dynamic filtration conditions. At static conditions, M8 membranes were kept in an ethanol solution for up to 4 days. Afterward, membrane permeance and salt rejection were examined and compared with the initial flux and salt rejection values. Stability tests in dynamic filtration conditions were performed by four consecutive filtration cycles (each about 180 h) at 2.0 bar operating pressure with a feed containing Milli-Q water spiked with ~45 μg L^{-1} of PFOA. Following each filtration cycle, the feed was replaced by ethanol for 6 h (similar filtration conditions). Following regeneration, the properties of the membranes were assessed (i.e., permeance and salt rejection).

MMCNF membrane regeneration experiments were carried out up to three consecutive cycles for PFOA spiked tap water using the same procedure used during the membrane stability test in dynamic filtration mode. PFOA spiked tap water (Composition: Ca^{2+}: 36 mg L^{-1}, Mg^{2+}: 8 mg L^{-1}, K^{+}: 1.7 mg L^{-1}, Na^{+}: 46.2 mg L^{-1}, Cl^{-}: 77 mg L^{-1}, S: 10 mg L^{-1}, pH: 7.7, Conductivity: 500 μS cm^{-1}, TOC: ~2 mg L^{-1}) collected from Midreshet Ben Gurion, Israel was used as feed during PFOA rejection and membrane regeneration experiments.

PFOA measurements

PFOA was analyzed using an Agilent Technologies LCMSMS, comprised of a 1260 Infinity II pump (model G7111B) coupled to a triple quadrupole (model G6465B) mass spectrometer and ESI source (Agilent Technologies Inc., Santa Clara, CA, USA). The system was adjusted to PFAS measurements using polypropylene tubes and aluminum filters for the eluent bottles and polypropylene vials with PFAS-free septas. A delay column was installed before the injector. The analytical column was ZORBAX RRHD Eclipse Plus C18, 2.1 × 100 mm, 1.8 μm (Part No. 959757-302). The binary solvent gradient consisted of (a) Milli-Q water with 5 mM Ammonium acetate and (b) 95% MeOH 5% water with 5 mM Ammonium-acetate. The gradient method conditions were: 0 min 10% B, 1.5 min 10% B, 3 min 30% B, 15 min 95% B, 15.5 min 100% B, 16.5 min 10% B, run ended at 21 min and had 7.5 min post-time. The flow rate was 0.4 mL min^{-1}, and the column temperature was 50 °C. Seven-point calibration curves were developed for each target analyte by diluting calibration stock at concentrations ranging from 1 to 100 ng mL^{-1}. All concentration levels were spiked with the internal standard at 10 ng mL^{-1}; the injection volume was 30 μL. Standards and samples were prepared in water. PFOA in experiment samples was identified by comparing chromatographic peak retention times and MRM parameters (specific qualifier and quantifier ions) with those of analytical standards. Quantification was done based on the response of PFOA in the sample relative to the internal-standard responses. Measurements were done on a negative ESI mode, with the gas temperature at 300 °C, gas flow at 15 L min^{-1}, nebulizer pressure at 15 psi, and capillary voltage at 2500 V. The ion source conditions for PFOA measurement included 69 V fragmentor and precursor ion m/z 413 for internal standard M8PFOA precursor ion m/z 421. Product ions for PFOA were m/z 369 and 169, with collision energies 3 V and 9 V, respectively. For the M8, the PFOA product ion was m/z 376 with collision energy 3 V.

DATA AVAILABILITY

Data generated or analyzed during this work is included in this manuscript and its supplementary information file. Raw data can be made available upon request from the authors.

Received: 14 April 2023; Accepted: 20 October 2023;
Published online: 07 November 2023

REFERENCES

1. Neuwald, I. J. et al. Ultra-Short-Chain PFASs in the sources of German drinking water: prevalent, overlooked, difficult to Remove, and unregulated. *Environ. Sci. Technol.* **56**, 6380–6390 (2022).
2. Das, S. & Ronen, A. A review on removal and destruction of per-and polyfluoroalkyl substances (PFAS) by novel membranes. *Membranes* **12**, 662 (2022).
3. Gagliano, E., Sgroi, M., Falciglia, P. P., Vagliasindi, F. G. A. & Roccaro, P. Removal of poly- and perfluoroalkyl substances (PFAS) from water by adsorption: Role of PFAS chain length, effect of organic matter and challenges in adsorbent regeneration. *Water Res.* **171**, 115381 (2020).
4. Glüge, J. et al. An overview of the uses of per- and polyfluoroalkyl substances (PFAS). *Environ. Sci. Process Impacts* **22**, 2345–2373 (2020).
5. Gar Alalm, M. & Boffito, D. C. Mechanisms and pathways of PFAS degradation by advanced oxidation and reduction processes: a critical review. *Chem. Eng. J.* **450**, 138352 (2022).
6. Bell, E. M. et al. Exposure, health effects, sensing, and remediation of the emerging PFAS contaminants – scientific challenges and potential research directions. *Sci. Total Environ.* **780**, 146399 (2021).
7. Cousins, I. T., Johansson, J. H., Salter, M. E., Sha, B. & Scheringer, M. Outside the safe operating space of a new planetary boundary for Per- and Polyfluoroalkyl Substances (PFAS). *Environ. Sci. Technol.* **56**, 11172–11179 (2022).
8. Johnson, J. K. et al. Removing forever chemicals via amphiphilic functionalized membranes. *NPJ Clean. Water* **5**, 55 (2022).
9. US EPA. *Proposed PFAS National Primary Drinking Water Regulation* (2023).
10. Lenka, S. P., Kah, M. & Padhye, L. P. A review of the occurrence, transformation, and removal of poly- and perfluoroalkyl substances (PFAS) in wastewater treatment plants. *Water Res.* **199**, 117187 (2021).
11. Gallen, C., Eaglesham, G., Drage, D., Nguyen, T. H. & Mueller, J. F. A mass estimate of perfluoroalkyl substance (PFAS) release from Australian wastewater treatment plants. *Chemosphere* **208**, 975–983 (2018).
12. Li, M. et al. Removal mechanisms of perfluorinated compounds (PFCs) by nanofiltration: Roles of membrane-contaminant interactions. *Chem. Eng. J.* **406**, 126814 (2021).
13. Olimattel, K., Zhai, L. & Sadmani, A. H. M. A. Enhanced removal of perfluorooctane sulfonic acid and perfluorooctanoic acid via polyelectrolyte functionalized ultrafiltration membrane: effects of membrane modification and water matrix. *J. Hazard. Mater. Lett.* **2**, 100043 (2021).
14. Soriano, A., Schaefer, C. & Urtiaga, A. Enhanced treatment of perfluoroalkyl acids in groundwater by membrane separation and electrochemical oxidation. *Chem. Eng. J. Adv.* **4**, 100042 (2020).

15. Franke, V., McCleaf, P., Lindegren, K. & Ahrens, L. Efficient removal of per- and polyfluoroalkyl substances (PFASs) in drinking water treatment: nanofiltration combined with active carbon or anion exchange. *Environ. Sci. Water Res. Technol.* **5**, 1836–1843 (2019).
16. Mastropietro, T. F., Bruno, R., Pardo, E. & Armentano, D. Reverse osmosis and nanofiltration membranes for highly efficient PFASs removal: overview, challenges and future perspectives. *Dalton Trans.* **50**, 5398–5410 (2021).
17. Xiong, J. et al. The rejection of perfluoroalkyl substances by nanofiltration and reverse osmosis: influencing factors and combination processes. *Environ. Sci. Water Res. Technol.* **7**, 1928–1943 (2021).
18. Boonya-Atichart, A., Boontanon, S. K. & Boontanon, N. Removal of perfluorooctanoic acid (PFOA) in groundwater by nanofiltration membrane. *Water Sci. Technol.* **74**, 2627–2633 (2016).
19. Boo, C. et al. High performance nanofiltration membrane for effective removal of perfluoroalkyl substances at high water recovery. *Environ. Sci. Technol.* **52**, 7279–7288 (2018).
20. Hang, X., Chen, X., Luo, J., Cao, W. & Wan, Y. Removal and recovery of perfluorooctanoate from wastewater by nanofiltration. *Sep. Purif. Technol.* **145**, 120–129 (2015).
21. Tang, W. et al. Preparation of hollow-fiber nanofiltration membranes of high performance for effective removal of PFOA and high resistance to BSA fouling. *J. Environ. Sci.* **122**, 14–24 (2022).
22. Wang, Y., Zucker, I., Boo, C. & Elimelech, M. Removal of emerging wastewater organic contaminants by polyelectrolyte multilayer nanofiltration membranes with tailored selectivity. *ACS EST Eng.* **1**, 404–144 (2021).
23. Pauletto, P. S. & Bandosz, T. J. Activated carbon versus metal-organic frameworks: a review of their PFAS adsorption performance. *J. Hazard. Mater.* **425**, 127810 (2022).
24. Wu, C., Klemes, M. J., Trang, B., Dichtel, W. R. & Helbling, D. E. Exploring the factors that influence the adsorption of anionic PFAS on conventional and emerging adsorbents in aquatic matrices. *Water Res.* **182**, 115950 (2020).
25. Alsbaiee, A. et al. Rapid removal of organic micropollutants from water by a porous β-cyclodextrin polymer. *Nature* **529**, 190–194 (2016).
26. Klemes, M. J. et al. Reduction of a tetrafluoroterephthalonitrile-β-cyclodextrin polymer to remove anionic micropollutants and perfluorinated alkyl substances from water. *Angew. Chem.* **131**, 12177–12181 (2019).
27. Ching, C., Klemes, M. J., Trang, B., Dichtel, W. R. & Helbling, D. E. β-Cyclodextrin polymers with different cross-linkers and ion-exchange resins exhibit variable adsorption of anionic, zwitterionic, and nonionic PFASs. *Environ. Sci. Technol.* **54**, 12693–12702 (2020).
28. Le, T., Jamshidi, E., Beidaghi, M. & Esfahani, M. R. Functionalized-MXene thin-film nanocomposite hollow fiber membranes for enhanced PFAS removal from water. *ACS Appl. Mater. Interfaces* **14**, 25397–25408 (2022).
29. Zhang, J., Huang, Z., Gao, L., Gray, S. & Xie, Z. Study of MOF incorporated dual layer membrane with enhanced removal of ammonia and per-/poly-fluoroalkyl substances (PFAS) in landfill leachate treatment. *Sci. Total Environ.* **806**, 151207 (2022).
30. Léniz-Pizarro, F. et al. Dual-functional nanofiltration and adsorptive membranes for PFAS and organics separation from water. *ACS EST Water* **2**, 863–872 (2022).
31. Jin, T. et al. Amyloid fibril-based membranes for PFAS removal from water. *Environ. Sci. Water Res. Technol.* **7**, 1873–1884 (2021).
32. Junker, M. A., Regenspurg, J. A., Valdes Rivera, C. I., Brinke, E. T. & de Vos, W. M. Effects of feed solution pH on polyelectrolyte multilayer nanofiltration membranes. *ACS Appl. Polym. Mater.* **5**, 355–369 (2022).
33. Elshof, M. G., de Vos, W. M., de Grooth, J. & Benes, N. E. On the long-term pH stability of polyelectrolyte multilayer nanofiltration membranes. *J. Memb. Sci.* **615**, 118532 (2020).
34. Lassalle, J. et al. Degradation of PFOS and PFOA in soil and groundwater samples by high dose electron beam technology. *Radiat. Phys. Chem.* **189**, 109705 (2021).
35. Baig, M. I., Willott, J. D. & de Vos, W. M. Enhancing the separation performance of aqueous phase separation-based membranes through polyelectrolyte multilayer coatings and interfacial polymerization. *ACS Appl. Polym. Mater.* **3**, 3560–3568 (2021).
36. Liu, C., Hatton, J., Arnold, W. A., Simcik, M. F. & Pennell, K. D. In situ sequestration of perfluoroalkyl substances using polymer-stabilized powdered activated carbon. *Environ. Sci. Technol.* **54**, 6929–6936 (2020).
37. Ramos, P. et al. Enhanced removal of per- and polyfluoroalkyl substances in complex matrices by polyDADMAC-coated regenerable granular activated carbon. *Environ. Pollut.* **294**, 118603 (2022).
38. Wan, H. et al. Gravity-driven electrospun membranes for effective removal of perfluoro-organics from synthetic groundwater. *J. Memb. Sci.* **644**, 120180 (2022).
39. Xiao, L. et al. β-Cyclodextrin polymer network sequesters perfluorooctanoic acid at environmentally relevant concentrations. *J. Am. Chem. Soc.* **139**, 7689–7692 (2017).
40. Khavani, M. et al. Effect of ethanol and urea as solvent additives on PSS-PDADMA Polyelectrolyte Complexation. *Macromolecules* **55**, 3140–3150 (2022).
41. Ilyas, S., de Grooth, J. & Nijmeijer, K. & De Vos, W. M. Multifunctional polyelectrolyte multilayers as nanofiltration membranes and as sacrificial layers for easy membrane cleaning. *J. Colloid Interface Sci.* **446**, 365–372 (2015).
42. Kamp, J. et al. Tuning the excess charge and inverting the salt rejection hierarchy of polyelectrolyte multilayer membranes. *J. Memb. Sci.* **639**, 119636 (2021).
43. Ghostine, R. A., Markarian, M. Z. & Schlenoff, J. B. Asymmetric growth in polyelectrolyte multilayers. *J. Am. Chem. Soc.* **135**, 7636–7646 (2013).
44. Chatterjee, S. & De, S. Adsorptive removal of arsenic from groundwater using a novel high flux polyacrylonitrile (PAN)-laterite mixed matrix ultrafiltration membrane. *Environ. Sci. Water Res. Technol.* **1**, 227–243 (2015).
45. Liu, C., Shi, L. & Wang, R. Enhanced hollow fiber membrane performance via semi-dynamic layer-by-layer polyelectrolyte inner surface deposition for nanofiltration and forward osmosis applications. *React. Funct. Polym.* **86**, 154–160 (2015).
46. Wu, Z. J. et al. Thin-film composite nanofiltration membrane modified by fulvic acid to enhance permeability and antifouling performance. *Ind. Eng. Chem. Res.* **61**, 8993–9003 (2022).

ACKNOWLEDGEMENTS

The authors thank the German Federal Ministry of Education and Research (BMBF; 02WIL1660A and 02WIL1660B) and the Israeli Ministry of Science and Technology (MOST) for funding within the German-Israeli Water Technology Cooperation Program. M.C. acknowledges the Kreitman School of Advance Studies for providing his postdoctoral fellowship. We thank CycloPure, Encinitas, CA, for providing the Dexsorb® powder for this research work.

AUTHOR CONTRIBUTIONS

M.C. contributed to the development and synthesis of the mixed-matrix nanofiltration membranes, filtration experiments design, conducting the experiments, writing the draft, and data analysis. M.S.A. contributed to developing the PFOA analysis methodology using LCMSMS, performing the analysis, quality assurance, and writing the methodology. A.R. contributed to methodology development, experimental design, review & editing, and funding acquisition. O.N. contributed to creating the concept, developing the methodology, experimental design, supervision, review & editing, writing the draft, and funding acquisition. All authors read and approved the final manuscript.

COMPETING INTERESTS

The authors declare no competing interests.

ADDITIONAL INFORMATION

Supplementary information The online version contains supplementary material available at https://doi.org/10.1038/s41545-023-00286-2.

Correspondence and requests for materials should be addressed to Avner Ronen or Oded Nir.

Reprints and permission information is available at http://www.nature.com/reprints

Publisher's note Springer Nature remains neutral with regard to jurisdictional claims in published maps and institutional affiliations.